3-25-2005

A Five-coordinate Metal Center in Co(II)-substituted VanX

Robert M. Breece
Miami University - Oxford

Alison L. Costello
University of New Mexico

Brian Bennett
Marquette University, brian.bennett@marquette.edu

Tara K. Sigdel
Miami University - Oxford

Megan L. Matthews
Miami University - Oxford

See next page for additional authors

THE JOURNAL OF BIOLOGICAL CHEMISTRY
Vol. 280, No. 12, Issue of March 25, pp. 11074–11081, 2005
Printed in U.S.A.

A Five-coordinate Metal Center in Co(II)-substituted VanX*

Received for publication, November 8, 2004, and in revised form, January 6, 2005
Published, JBC Papers in Press, January 17, 2005, DOI 10.1074/jbc.M412582200

Robert M. Breece‡, Alison Costello§, Brian Bennett¶, Tara K. Sigdel‡, Megan L. Matthews‡, David L. Tierney§, and Michael W. Crowder‡‖

From the ‡Department of Chemistry and Biochemistry, Miami University, Oxford, Ohio 45056, §Department of Chemistry, University of New Mexico, Albuquerque, New Mexico 87131-0001, and ¶National Biomedical EPR Center, Department of Biophysics, Medical College of Wisconsin, Milwaukee, Wisconsin 53226-0509

In an effort to structurally probe the metal binding site in VanX, electronic absorption, EPR, and extended x-ray absorption fine structure (EXAFS) spectroscopic studies were conducted on Co(II)-substituted VanX. Electronic spectroscopy revealed the presence of Co(II) ligand field transitions that had molar absorptivities of ~100 M^{-1} cm^{-1}, which suggests that Co(II) is five-coordinate in Co(II)-substituted VanX. Low temperature EPR spectra of Co(II)-substituted VanX were simulated using spin Hamiltonian parameters of $M_S = |\pm ½\rangle$, E/D = 0.14, $g_{real(x,y)}$ = 2.37, and $g_{real(z)}$ = 2.03. These parameters lead to the prediction that Co(II) in the enzyme is five-coordinate and that there may be at least one solvent-derived ligand. Single scattering fits of EXAFS data indicate that the metal ions in both native Zn(II)-containing and Co(II)-substituted VanX have the same coordination number and that the metal ions are coordinated by 5 nitrogen/oxygen ligands at ~ 2.0 Å. These data demonstrate that Co(II) (and Zn(II) from EXAFS studies) is five-coordinate in VanX in contrast to previous crystallographic studies (Bussiere, D. E., Pratt, S. D., Katz, L., Severin, J. M., Holzman, T., and Park, C. H. (1998) *Mol. Cell* 2, 75–84). These spectroscopic studies also demonstrate that the metal ion in Co(II)-substituted VanX when complexed with a phosphinate analog of substrate D-Ala-D-Ala is also five-coordinate.

Vancomycin is a cup-shaped glycopeptide that has been called the "antibiotic of last resort" (1, 2) because it is often used for antibiotic-resistant bacterial infections and in patients who are allergic to penicillins. Vancomycin inhibits bacterial cell wall synthesis by binding to the D-Ala-D-Ala end of the peptidoglycan pentapeptide via five hydrogen bonds, thereby preventing cross-linking of the cell wall precursors (3–6). However, bacterial resistance to vancomycin in human pathogens has emerged, particularly in *Enterococcus* and *Staphylococcus* strains (3–6). The genes responsible for inducible, high level vancomycin resistance are carried on a 10-kb transposon, which can be converted into self-transferable plasmids and transferred by conjugation (7). The activities of five gene products are required for high level resistance: VanR, VanS, VanH, VanA, and VanX (5). VanR and VanS make up a two-component, signal transduction system that regulates the expression of the other three genes and appears to be stimulated by the presence of vancomycin (8–10). VanH encodes for a D-specific α-ketoacid reductase, which catalyzes the reduction of pyruvate into D-lactate using NADPH (11, 12). VanA is a ligase that uses the D-lactate produced by VanH and generates a D-Ala-D-lactate depsipeptide (11, 13). This depsipeptide is added to a sugar-linked tripeptide by MurF, producing a modified bacterial cell wall precursor that can be incorporated into the growing peptidoglycan layer by the normal bacterial enzymes (3, 5, 12). Vancomycin binds to this modified cell wall pentapeptide 10^3 less tightly than to the normal pentapeptide due to the loss of one hydrogen bond and to a key electrostatic repulsion (11, 14, 15). In other words, bacteria modify their peptidoglycan layers to reduce the binding affinity of vancomycin, thereby making the bacterium resistant to vancomycin.

The final gene product, VanX, is a D-Ala-D-Ala peptidase (16). Walsh and co-workers (17–21) have reported the cloning, overexpression, and purification of VanX. VanX is a Zn(II)-binding protein with a monomeric molecular mass of 23,365 Da that hydrolyzes a very narrow range of substrates and does not hydrolyze D-Ala-D-lactate or D-Ala-L-Ala (16, 17). Walsh and co-workers (18) used site-directed mutagenesis studies to predict the metal binding amino acids, and these predictions were confirmed when Bussiere and co-workers (1) published the crystal structure of VanX. The mutagenesis study also implicated Arg-71 and Glu-181 as having roles in catalysis, and these residues were shown in the crystal structure to be close to the Zn(II) ion. The crystal structure also revealed that VanX crystallized as a homohexamer, and each subunit bound one Zn(II). The Zn(II) ion was coordinated in a distorted tetrahedral arrangement with the side chains of His-116, His-184, and Asp-123 and a solvent water as ligands (Fig. 1). The crystal structure also demonstrated a narrow cavity leading to the active site (1), which nicely explained the very narrow substrate specificity of VanX.

Since VanX is essential for vancomycin resistance in bacteria, the enzyme has been targeted for drug/inhibitor design studies in hopes that an inhibitor can be given in combination with vancomycin as a treatment for vancomycin-resistant bacterial infections. Phosphinate and phosphonate analogs of D-Ala-D-Ala have been shown to be inhibitors of VanX, suggesting that the enzyme utilizes a nucleophile-driven hydrolysis reaction that may proceed via a tetrahedral transition state intermediate (17, 22, 23). However, these structurally similar compounds exhibit K_i values varying over several orders of magnitude, and the crystal structure of VanX complexed with a phosphonate and a phosphinate demonstrated two distinct binding interactions (1). Wu and Walsh (24) reported several

* This work was supported by National Institutes of Health Grants AI40052 and GM40052 (to M. W. C.) and AI056231 and EB001980 (to B. B.) and American Chemical Society Petroleum Research Fund Grant G3-39200 (to D. L. T.). The National Synchrotron Light Source was supported by the United States Department of Energy. The costs of publication of this article were defrayed in part by the payment of page charges. This article must therefore be hereby marked "*advertisement*" in accordance with 18 U.S.C. Section 1734 solely to indicate this fact.

‖ To whom correspondence should be addressed: Dept. of Chemistry and Biochemistry, Miami University, 112 Hughes Hall, Oxford, OH 45056. Tel.: 513-529-7274; Fax: 513-529-5715; E-mail: crowdemw@muohio.edu.

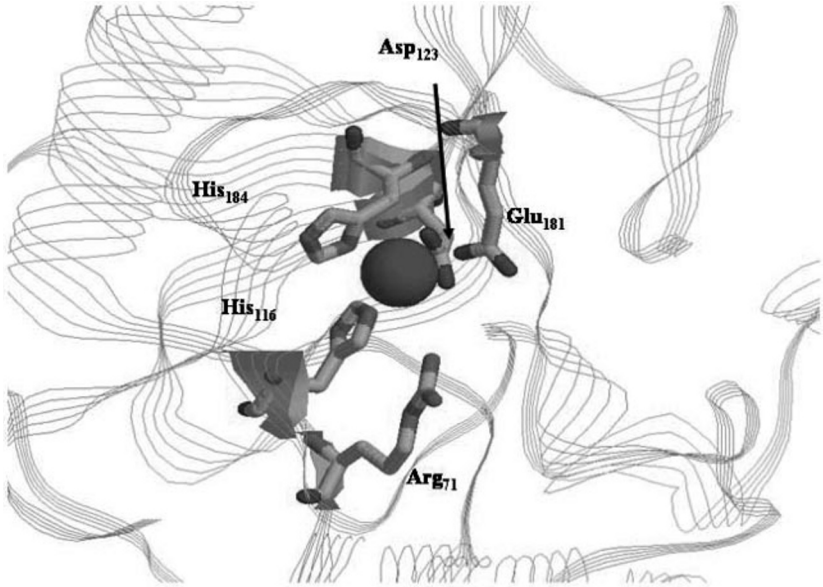

FIG. 1. **Active site of VanX (1).** The figure was rendered by Rasmol version 2.6.

dithiol compounds that exhibited potent, time-dependent inhibition of VanX, and Araoz *et al.* (25) reported that a modified D-Ala-D-Gly dipeptide is a mechanism-based inactivator of VanX. The former compounds apparently inhibit VanX by chelating Zn(II) and blocking access of the substrate. The latter compound, upon hydrolysis by VanX, releases a reactive 4-thioquinonefluoromethide that reacts with a group on the surface of the enzyme. Unfortunately none of the reported inhibitors bind tightly enough or are specific enough to be useful as clinical inhibitors.

One of the major obstacles in studying VanX is the lack of a direct activity assay. The inability to find chromogenic substrates for VanX is presumably due to the narrow binding cavity in the enzyme that leads up to the active site. The lack of a direct activity assay complicates mechanistic studies, results from which could drive rational inhibitor design or redesign efforts. A ninhydrin-based assay, a capillary electrophoresis procedure, and several coupled assays have been reported (17, 25–27); however, all of these have experimental problems that limit their use in mechanistic studies. As an alternative, we propose to follow the mechanism by preparing the Co(II)-substituted form of VanX and probing the spectroscopic properties of the metal center during the catalytic cycle with use of stopped-flow and rapid freeze quench coupled with spectroscopic studies. This work describes the preparation of Co(II)-VanX and the biochemical and spectroscopic characterization of the resulting enzyme.

MATERIALS AND METHODS

Preparation of Co(II)-substituted Maltose-binding Protein-VanX and VanX—Co(II)-substituted maltose-binding protein (MBP)[1]-VanX and VanX were prepared in minimal medium. The minimal medium contained 2.5 g/liter D-(+)-glucose, 5 g/liter casamino acids, 10.8 g/liter K_2HPO_4, 5.5 g/liter KH_2PO_4, 10 g/liter NaCl, 1 g/liter $(NH_4)_2SO_4$, 2 mg/liter thiamine, 1 mg/liter biotin, and a 1 ml/liter concentration of a metal mixture containing 124 mg/liter $MgSO_4 \cdot 7H_2O$, 74 μg/ml $CaCl_2 \cdot 2H_2O$, 20 μg/ml $MnCl_2 \cdot 4H_2O$, 31 μg/ml H_3BO_3, 1.2 μg/ml $(NH_4)_6Mo_7O_{24} \cdot 4H_2O$, and 1.6 μg/ml $CuSO_4$ (28). In early preparations the buffered medium was adjusted to pH 7.5 following a previously reported protocol (28), but in later preparations, the medium was adjusted to pH 6.8 to increase the yields of Co(II)-VanX.

Plasmid pIADL14, containing the gene that encodes for a MBP-VanX fusion protein (MBP-VanX), was a gift from Professor Christopher Walsh at Harvard Medical School (18). The plasmid was transformed into BL21(DE3) *Escherichia coli* cells, and colonies containing the plasmid were selected on Luria-Bertani (LB) agar plates containing 25 μg/ml kanamycin. A single colony from this plate was used to make an overnight preculture in minimal medium containing 25 μg/ml kanamycin. Three 1-liter flasks, each containing 333 ml of minimal medium and 25 μg/ml kanamycin, were inoculated with 10 ml of the overnight preculture and were allowed to grow to an $A_{600\ nm}$ of 1.6–1.8 at 30 °C. Protein production was induced by making the cultures 1 mM in isopropyl β-D-thiogalactopyranoside. At induction, the cultures were also made 100 μM in $CoCl_2$. The cells were then collected by centrifugation for 15 min at 8,275 $\times$ *g*, flash frozen in liquid N_2, and stored at −80 °C overnight.

The cell pellets were thawed on ice and were resuspended in 30 mM Tris-HCl, pH 7.6, containing 200 mM NaCl. Cells were lysed by passing the resuspension two times through a French press at 16,000 p.s.i., and the cellular debris were collected by centrifugation for 15 min at 32,583 $\times$ *g*. The cell lysate was then loaded on a 60-ml amylose column (26 mm $\times$ 20 cm), and protein was eluted with a 0–10 mM maltose gradient over 300 ml in 30 mM Tris-HCl, pH 7.6, containing 200 mM NaCl. Fractions containing MBP-VanX were identified by SDS-polyacrylamide gels, and pure fractions were pooled and concentrated to ~10 ml with an Amicon ultrafiltration concentrator equipped with a YM-10 membrane. This overexpression/purification protocol resulted in 40 mg of MBP-VanX fusion protein/liter of growth culture. The maltose-binding protein from the fusion MBP-VanX protein was removed by thrombin digestion. Three units of restriction grade thrombin were added for every 1 mg of uncleaved MBP-VanX, and the cleavage was allowed to incubate for 10 h in a water bath at 25 °C. The cleaved proteins were then separated by two methods: a 120-ml Sephacryl S-200 HR size exclusion column (16 mm $\times$ 60 cm) or a 25-ml Q-Sepharose anion exchange column (16 mm $\times$ 20 cm).

Fractions containing purified, cleaved VanX, as judged by SDS-PAGE, were pooled and concentrated using an Amicon ultrafiltration concentrator equipped with a YM-10 membrane. VanX concentrations were determined by using the sample's absorbance at 280 nm, the extinction coefficient ($\epsilon_{280\ nm}$), and Beer's Law. The extinction coefficients of MBP-VanX ($\epsilon_{280\ nm}$ = 115,700 $M^{-1}\ cm^{-1}$) and VanX ($\epsilon_{280\ nm}$ = 51,200 $M^{-1}\ cm^{-1}$) were determined with amino acid analyses performed at the Protein Separation and Analysis Laboratory in the Department of Biochemistry at Purdue University.

Steady-state Kinetic Studies—Steady-state kinetics were performed using a coupled assay developed for VanX by Badet and co-workers (25). This assay involves the use of other enzymes, such as D-lactate dehydrogenase (Sigma), catalase (Sigma), and D-amino-acid oxidase (Calzyme Laboratories). All enzymes other than VanX were kept in excess so the rate-limiting process in the coupled reactions is the formation of D-Ala by VanX. All reactions were conducted at 37 °C on an Agilent 8453 UV-visible spectrophotometer. Concentrations of reagents used in the coupled assay were as follows: VanX at 1–5 nM, D-lactate dehydrogenase at 57 units/ml, catalase at 520 units/ml, D-amino-acid oxidase at 1.2 units/ml, NADH at 10 mM, and D-Ala-D-Ala was varied from 50 μM

[1] The abbreviations used are: MBP, maltose-binding protein; EXAFS, extended x-ray absorption fine structure; ICP-AES, inductively coupled plasma with atomic emission spectroscopy.

to 2 mM with all solutions being made in 50 mM Hepes, pH 8.0, containing 200 mM NaCl. The reactions were monitored at 340 nm, and the reactions were designed to ensure the loss of ~1 absorbance unit over the course of 10 min. Absorbance values for the linear portion of the curves were converted into velocities using the molar extinction coefficient for NADH ($\epsilon_{340\ nm}$ = 6,220 M^{-1} cm^{-1}) and the time interval of the absorbance change. These values were then plotted against the corresponding substrate concentrations, and the resulting plots were fitted to the Michaelis-Menten equation $v_o = V_{max}[S]/(K_m + [S])$ using Igor Pro version 4.05A.

Metal Analyses—Metal analyses were performed using a Varian Liberty 150 ICP-AES spectrometer. All purified enzyme samples were diluted to ~10 μM with 30 mM Tris-HCl, pH 7.6. A calibration curve with four standards and a correlation coefficient of greater than 0.999 was generated using serial dilutions of Fisher metal standards. Three trials of each sample were averaged. The following wavelengths for the indicated metal ions were used to ensure the lowest detection limit possible: zinc, 213.856 nm; copper, 324.754 nm; nickel, 321.604 nm; cobalt, 238.892 nm; iron, 259.940 nm; and manganese, 257.610 nm.

Size Exclusion Chromatography—A 120-ml Sephacryl S-200 HR size exclusion column was used to determine the molecular masses of MBP-VanX and VanX. A calibration curve was used to relate molecular weight to the retention time. The standard proteins were blue dextran 2000 (molecular mass, 2 MDa), thyroglobulin (molecular mass, 669 kDa), ferritin (molecular mass, 440 kDa), catalase (molecular mass, 232 kDa), aldolase (molecular mass, 158 kDa), and albumin (molecular mass, 67 kDa). The mobile phase buffer was 0.05 M Na_3PO_4, pH 7.6, containing 150 mM NaCl, and the flow rate was 0.5 ml/min. Analysis of protein location was conducted using UV-visible spectroscopy measuring the absorbance at 280 nm of every 2-ml fraction.

UV-Visible Spectroscopy—All UV-visible spectra were collected on an Agilent 8453 UV-visible spectrophotometer with photodiode array detection measuring the UV-visible absorbance at each wavelength between 200 and 1,100 nm. Enzyme concentrations ranged from 200 μM to 1 mM, and enzyme samples were loaded in a 0.5-ml quartz cuvette. The buffer used for dilutions and for the blanks was 30 mM Tris-HCl, pH 7.6. Spectra were recorded at 25 °C. The phosphinate inhibitor (22, 23) D-3-[(1-aminoethyl)phosphinyl]-2-methylpropionic acid was synthesized by Dr. Ke-Wu Yang and was dissolved in 50 mM Hepes, pH 8.0. The solution of inhibitor was added directly to the VanX samples.

EPR Spectroscopy—All EPR spectra were obtained on a Bruker Instruments ER 300 EPR spectrometer equipped with an ER 035M NMR gaussmeter and a Hewlett Packard 5352B microwave frequency counter. Spectra were recorded at various temperatures between 4 and 16 K using an Oxford Instruments liquid helium-cooled cryostat. Spectra were recorded with the following conditions: 2-milliwatt microwave power, 9.48-GHz microwave frequency, and 10-G modulation amplitude at 100 kHz. Conditions were chosen so as to be non-saturating. Spectra were integrated, and the base line was examined to verify that spectral distortion due to passage effects did not occur. Samples in solution were pipetted into 4-mm outer diameter quartz EPR tubes and then flash frozen in liquid nitrogen. Precipitated VanX samples were centrifuged, and the supernatant was decanted. A small volume of 30 mM Tris, pH 7.6, was added, and the solid was resuspended. The resulting slurry was then pipetted into an EPR tube and flash frozen.

EPR spectra were simulated with the program XSophe (Bruker), assuming a spin Hamiltonian $H = \beta g \cdot S \cdot H + S \cdot D \cdot S$ with $S = 3/2$ and where $D > 0$ corresponds to an $M_S = |\pm ½\rangle$ ground state Kramers' doublet. For Co(II), $|D|$ is usually much greater than the Zeeman interaction (29); with $|D| \gg \beta gSH$, the simulations are insensitive to the precise magnitude of D and an arbitrary value of D = 50 cm^{-1} was assumed. The useful EPR parameters that can be extracted from the simulations are g_{real} and E/D (30).

X-ray Absorption Spectroscopy—MBP-VanX samples were concentrated to ~1 mM using ultrafiltration and were prepared with 30% (v/v) added glycerol as glassing agent. Samples were loaded in Lucite cuvettes with 6-μm polypropylene windows and frozen rapidly in liquid nitrogen. X-ray absorption spectra were measured at the National Synchrotron Light Source, beamline X9B, with a silicon(111) double crystal monochromator; harmonic rejection was accomplished using a curved nickel focusing mirror. Fluorescence excitation spectra for all samples were measured with a 13-element solid-state germanium detector array. The detectors were run at a total incident count rate of <100 kHz per channel with fluorescence count rates (K_α) of ~ 1.5 kHz per channel. Samples were held at or below 15 K in a Displex cryostat during X-ray absorption spectroscopy measurements. EXAFS spectra were measured with 10-eV steps below the edge, 0.5-eV steps in the edge region, and 0.05-$Å^{-1}$ steps in the EXAFS region. Integration times varied from 1 s in the pre-edge region to 13 s at $k \approx 12$ $Å^{-1}$. X-ray energies were calibrated by reference to the absorption spectrum of the appropriate metal foil measured concurrently with protein spectra. The first inflection point of the metal foil was assigned as the K_α binding energy: 7,709 eV for cobalt and 9,659 eV for zinc.

Data were processed using SixPack (SixPack is available free of charge from www-ssrl.slac.Stanford.edu/~swebb/sixpack.htm). Both fluorescence and incident count rates from each detector channel were examined, to confirm the absence of artifacts, prior to averaging. Final spectra were obtained by averaging four to six scans per sample with the inclusion of 10–12 detector channels per scan. Background subtraction included a Gaussian pre-edge, centered at approximately the K_α fluorescence energy, and a three-region spline of fourth order in the EXAFS region. Data were converted from energy to k space using $k = \sqrt{2m_e(E - E_0)/\hbar^2}$ with E_0 set at 7,745 eV (cobalt) or 9,675 eV (zinc). Resultant EXAFS spectra were Fourier-transformed over the range k = 1–12.1 $Å^{-1}$ (cobalt) or 1–13.6 $Å^{-1}$ (zinc). The first shell (r = 0.6–2.2 Å (cobalt), r = 0.7–2.1 Å (zinc)) was reverse Fourier-transformed over the same k range. The Fourier-filtered first shell EXAFS (~10 degrees of freedom) data were fitted to Equation 1 using the nonlinear least-squares engine of IFEFFIT (IFEFFIT is available free of charge from cars9.uchicago.edu/ifeffit and is distributed with SixPack).

$$\chi(k) = \sum \frac{N_{as}A_s(k)S_c}{kR_{as}^2} \exp(-2k^2\sigma_{as}^2)\exp(-2R_{as}/\lambda)\sin[2kR_{as} + \phi_{as}(k)] \qquad \text{(Eq. 1)}$$

In Equation 1, N_s is the number of scattering atoms within a given radius ($R_{as} \pm \sigma$), $A_s(k)$ is the backscattering amplitude of the absorber-scatterer (as) pair, $\phi_{as}(k)$ is the phase shift experienced by the photoelectron as it encounters the electron clouds of the scattering and absorbing atoms, λ is the photoelectron mean free path, and the sum is taken over all shells of scattering atoms. Theoretical amplitude and phase functions, $A_s(k)\exp(-2R_{as}/\lambda)$ and $\phi_{as}(k)$, were calculated using FEFF version 8.00 (31). Optimal absorber-scatterer-specific scale factors, S_c, were determined by fitting experimental spectra for compounds of known structure (0.78 for Co—N from cobalt(II) trispyrazolylborate (32) and 0.74 for Zn—N from zinc(II) tetrakisimidazole (33)). Fits to protein data were then obtained for all reasonable integer coordination numbers holding S_c fixed and allowing ΔE_o, R_{as}, and σ_{as}^2 to vary. The best all nitrogen fits are summarized in Table II. Similar results were obtained using a single shell of oxygen atoms to model the first shell. Markedly better fit residuals were obtained with mixed nitrogen/oxygen models; however, the data do not possess sufficient degrees of freedom to warrant the use of multiple atom types, and these fits are not reported.

RESULTS

Preparation and Characterization of Co(II)-substituted VanX—Our initial efforts to prepare Co(II)-substituted VanX involved using the direct addition method as described by Auld (34, 35). In our case, this method involved the removal of naturally occurring Zn(II) by dialysis *versus* chelators and the addition of Co(II) to apoVanX. Despite considerable efforts, we could not use this method to prepare Co(II)-substituted VanX in concentrations sufficient for spectroscopic studies as the protein precipitated during dialysis and concentration steps, and frequently Co(II) oxidized to Co(III) during the steps.

Therefore, a biosynthetic method to prepare Co(II)-substituted VanX was used (28, 35). By using a previously published method for the preparation of VanX as a fusion protein with MBP (18), Co(II)-substituted VanX was overexpressed in minimal medium supplemented with 100 μM $CoCl_2$ and purified using an amylose affinity column. The MBP-VanX fusion protein was cleaved with thrombin, and the cleaved proteins were separated by using size exclusion or ion-exchange chromatography. VanX eluted from the size exclusion column earlier than MBP despite VanX having a monomeric molecular mass of 23 kDa and MBP having a molecular mass of 42 kDa. This result suggests that VanX aggregates in solution into a species with a molecular mass greater than 42 kDa. To further test this hypothesis, size exclusion chromatography was used to determine the quaternary structures of VanX and MBP-VanX. Both proteins eluted from the column right after blue dextran and had elution times consistent with molecular masses of 500 and 630

TABLE I
Steady-state kinetic constants and metal content of VanX samples
Steady-state kinetic constants were determined using the coupled assay (25), and metal content was determined by ICP-AES.

Enzyme	k_{cat}	K_M	Metal Content	Source
	s^{-1}	μM	*eq*	
Zn(II)-VanX	41 ± 2	110 ± 10	NR[a] 0.87[b] Zn(II)	Ref. 25
Zn(II)-VanX	156 ± 16	109 ± 40	0.70 ± 0.02 Zn(II)	Our data
Co(II)-VanX	94 ± 6	140 ± 40	0.06 ± 0.03 Zn(II) 0.60 ± 0.09 Co(II)	Our data
MBP-Co(II)-VanX	110 ± 20	100 ± 40	0.06 ± 0.03 Zn(II) 0.66 ± 0.09 Co(II)	Our data

[a] Not reported.
[b] Reported in Ref. 18.

kDa, respectively. The elution profile was unaffected by the inclusion of dithiothreitol or higher concentrations of salt in the buffer. The result with the reductant was not surprising since the crystal structure of hexameric VanX showed that disulfides are not involved in the aggregation of VanX.[2] This result suggests that MBP-VanX, in the buffers and at the concentrations used in our studies, has a decameric structure, while VanX is composed of over 20 monomers. Efforts to concentrate these samples show that MBP-VanX can be concentrated to 1.6 mM, while VanX can only be concentrated to 0.3 mM.

The steady-state kinetic properties of Co(II)-substituted VanX and MBP-VanX were determined using the optimized coupled assay of Badet and co-workers (25) (Table I). Co(II)-substituted VanX exhibited k_{cat} and K_m values of 94 ± 6 s^{-1} and 140 ± 40 μM, respectively, and these values were similar to those of the fusion protein Co(II)-MBP-VanX (k_{cat} = 110 ± 20 s^{-1} and K_m = 100 ± 40 μM). It is clear that the presence of MBP does not affect the steady-state kinetic constants exhibited by VanX in agreement with previous reports (18). The Co(II)-substituted analogs of VanX exhibited K_m values identical to Zn(II)-VanX and a 70% reduction in k_{cat} values, which is common for Co(II)-substituted enzymes (36). In our experiments, the k_{cat} value for Zn(II)-VanX was 3-fold higher than that previously reported (25). It is possible, in the previous report (25), the rate of D-amino-acid oxidase contributed to the overall rate of reaction attributed to VanX.

Metal analyses on VanX produced from the MBP fusion construct showed that the isolated enzymes bind roughly 0.70 ± 0.02 equivalents of only cobalt or zinc. No other metal ions were found in the VanX samples. The inclusion of higher concentrations of Zn(II)/Co(II) in the growth medium used for overexpression did not result in purified VanX samples with more equivalents of metal ions. If excess Zn(II) or Co(II) was added to the as-isolated VanX (or MBP-VanX) and the enzymes were exhaustively dialyzed *versus* metal-free buffer, the resulting enzymes contained 1.0 ± 0.1 metal ion per monomer. We were unable to isolate Co(II)-substituted VanX that contained less than 0.06 equivalents of Zn(II), most likely due to Zn(II) from buffers, growth medium, glassware, etc.

Electronic Spectra of Co(II)-substituted VanX—The UV-visible spectrum of Co(II)-substituted MBP-VanX shows three peaks at 520, 550, and 580 nm and no other features above 300 nm (Fig. 2*A*). The peak at 580 nm often appears as a shoulder of the 550 nm peak. These peaks have molar extinction coefficients of ~100 M^{-1} cm^{-1}, suggesting these transitions are ligand field transitions of high-spin Co(II) and that the Co(II) ion is five-coordinate (37). There were no peaks at ~320 nm in any of the UV-visible spectra of Co(II)-substituted VanX, suggesting that Co(II) does not bind to either of the solvent-accessible cysteines in VanX (38–40).

[2] C. H. Park, personal communication.

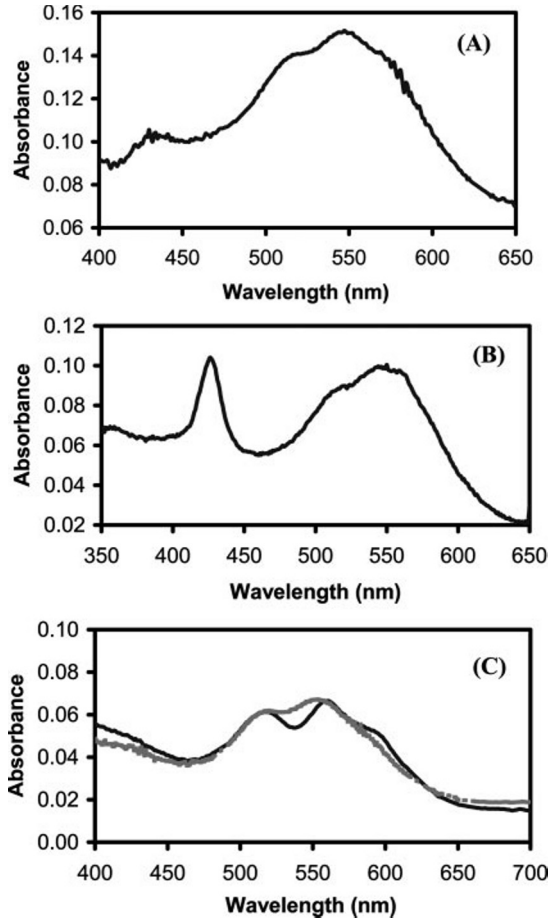

FIG. 2. **UV-visible difference spectrum in 50 mM Tris, pH 7.6, of 0.8 mM Co(II)-substituted MBP-VanX prepared in minimal medium at pH 6.8 (*A*), 0.8 mM Co(II)-substituted MBP-VanX prepared in minimal medium at pH 7.5 (*B*), and 0.6 mM Co(II)-substituted MBP-VanX (*gray line*) and 0.6 mM Co(II)-substituted MBP-VanX with 0.6 mM phosphinate (*black line*) (*C*).**

When Co(II)-substituted MBP-VanX was prepared in minimal medium, pH 7.5, the resulting enzyme exhibited similar ligand field transitions as in Fig. 2*A*; however, an additional feature at 425 nm that had an extinction coefficient of ~100 M^{-1} cm^{-1} was observed (Fig. 2*B*). The intensity of this peak implies that it is due to a ligand field transition rather than from a ligand to metal charge transfer band (expected ϵ of >500 M^{-1} cm^{-1}) (40). The position of this peak suggests that it arises from Co(III) in the sample, indicating that Co(II) is air-oxidizing to Co(III) during protein preparation at pH 7.5. The preparation of Co(II)-substituted VanX in minimal medium, pH 6.8, reduces the amount of air oxidation (Fig. 2*A*).

In an effort to extend the use of UV-visible spectroscopy to

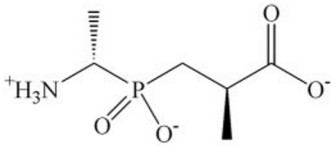

FIG. 3. **Structure of phosphinate analog of D-Ala-D-Ala.**

probe inhibitor binding to VanX, UV-visible spectra were collected on samples of Co(II)-substituted MBP-VanX complexed with the phosphinate analog of D-Ala-D-Ala (Fig. 3). Previously Walsh and co-workers (23) reported that this phosphinate is a slow binding inhibitor of VanX with a K_i value of 1.26 μM. Therefore, a 0.5 mM Co(II)-MBP-VanX sample containing equimolar equivalents of phosphinate inhibitor was expected to result in ~100% enzyme-inhibitor complex. In addition, Bussiere and co-workers (1) published a crystal structure of the Zn(II)-VanX-phosphinate complex; this structure showed that both phosphinate oxygens coordinate Zn(II) and that Zn(II) is five-coordinate. Based on this crystal structure and our data on uncomplexed Co(II)-MBP-VanX, we hypothesized that the intensities of the Co(II) ligand field transitions would be the same as those of the uncomplexed enzyme. In addition, we hypothesized that the peak positions of the ligand field transitions would shift to slightly longer wavelengths since the phosphinate oxygens were expected to be weaker field ligands than water. The UV-visible spectrum of Co(II)-MBP-VanX complexed with the phosphinate inhibitor is shown in Fig. 2*C*. As hypothesized, the intensities of the ligand field transitions in uncomplexed and complexed VanX are the same, suggesting that Co(II) is five-coordinate in both spectra (37). The simplest explanation for this observation is that the phosphinate oxygens replace two solvent molecules in the complexed enzyme. However, we cannot rule out the possibility that binding of the phosphinate results in the loss of one solvent molecule and the "shifting" of a chelating Asp-123 to a monodentate binding mode. This behavior has been reported previously for iron enzymes and has been called the "carboxylate shift" (41). Efforts to obtain the crystal coordinates of the VanX-phosphinate complex were unsuccessful as these data are no longer available.[2]

EPR Spectra of Co(II)-substituted VanX—Initially we attempted to utilize unfused VanX in EPR studies; however, when we concentrated these samples, VanX precipitated. The precipitated protein could be diluted with buffer and resolubilized, but the final concentration of soluble VanX was never greater than 0.3 mM. We, therefore, collected EPR spectra on precipitated VanX and soluble MBP-VanX samples at 8 K. The 1.6 mM Co(II)-MBP VanX sample exhibited an EPR signal with turning points at $g_{eff(x,y,z)}$ = 1.92, 3.71, and 5.64 (Fig. 4*C*). Computer simulation (Fig. 4*D*) returned spin Hamiltonian parameters of $M_S = |\pm ½\rangle$, E/D = 0.14, $g_{real(x,y)}$ = 2.37, and $g_{real(z)}$ = 2.03 (Fig. 4*D*). These parameters are not dissimilar to those from other Co(II)-containing proteins (29, 42) and are indicative of either a five- or six-coordinate Co(II) center (43). Six-coordinate Co(II) ions typically exhibit low E/D due to the high degree of axial symmetry, particularly when unconstrained ligands such as water allow for geometric relaxation, and examples of this include $Co(H_2O)_6^{2+}$ and the methionyl aminopeptidase from *E. coli* (44). The E/D value for VanX, however, is intermediate for Co(II) centers that are axially symmetric ($E/D \sim 0$) and for those with the lowest possible degree of axial symmetry (E/D = ⅓) (30). Thus, the EPR data, especially when considered along with the extinction coefficients of the electronic absorption ligand field transitions, suggest that the coordination number of Co(II) in Co(II)-MBP-VanX is five (29). For five-coordinate systems with no solvent-derived ligands, such as the leucine phosphonic acid complex of the aminopeptidase from *Vibrio proteolyticus*, E/D is significantly higher (0.26) than for VanX, and the moderate E/D (0.14) for VanX may signify the presence of at least one solvent-derived ligand.

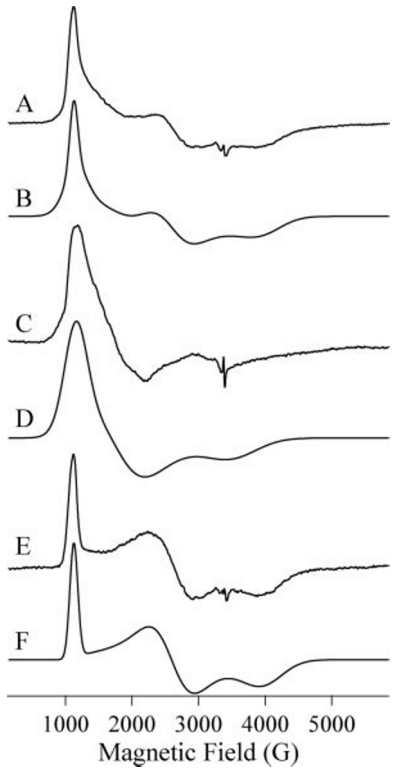

FIG. 4. **EPR simulation of 1.6 mM Co(II) MBP-VanX and precipitated Co(II) MBP-VanX at 8 K.** *Spectrum A* is the measured spectrum of the precipitated enzyme. *Spectrum C* is the measured spectrum of the 1.6 mM enzyme. *Spectrum E* is the subtraction of *spectrum C* from *spectrum A*. *Spectra D* and *F* are the simulations of *spectra C* and *E*, respectively. *Spectrum B* is the sum of *spectra D* and *F*.

The EPR spectrum of precipitated Co(II)-VanX contains a component that exhibits markedly higher rhombic distortion of the axial zero field splitting than that of soluble Co(II)-substituted MBP-VanX and is similar to spectra reported for Co(II)-substituted carboxypeptidase A (Fig. 4*A*) (42). The spectrum of precipitated Co(II)-VanX appears to result from two components (Fig. 4*E*, see difference spectrum). The minor component is indistinguishable from soluble Co(II)-substituted MBP-VanX (Fig. 4, *C* and *E*) and is presumably due to the soluble fraction of Co(II)-VanX. The major component has g_{eff} values of around 1.69, 2.57, and 5.92 (Fig. 4*E*). The simulation of *spectrum E* (Fig. 4) indicates values of E/D = 0.277, $g_{real(x,y)}$ = 2.235, and $g_{real(z)}$ = 2.112 (Fig. 4*F*). The similar values of $g_{(x,y)} - g_{(z)}$ for both the soluble MBP-VanX and the precipitated VanX suggest that there is no marked pseudotetragonal elongation or compression in going from the solution phase to the precipitate, but the higher E/D value for the precipitated VanX indicates a decrease in axial electronic symmetry, and the narrower lines suggest a loss of conformational flexibility of the Co(II)-coordinating ligands. These phenomena are consistent with a solvent ligand being replaced by a rigid ligand and therefore may be due to Asp-123 providing a bidentate ligand to the metal center in the precipitated form with the second carboxylate oxygen atom replacing a coordinated water. The chelate binding mode of an Asp/Glu residue is precedented in carboxypeptidase A (45).

The EPR spectrum of the precipitated Co(II)-VanX with bound phosphinate was essentially due to a single species. The spectrum exhibited turning points at g_{eff} values of 1.86, 2.87, and 5.78, and computer simulation returned values of E/D =

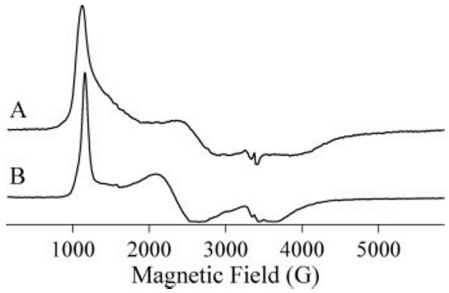

FIG. 5. **Comparison of two solid VanX spectra without (*A*) and with (*B*) phosphinate inhibitor added.**

0.233, $g_{(x,y)} = 2.245$, and $g_{(z)} = 2.165$ with an M_S value of $|\pm\frac{1}{2}\rangle$ (Fig. 5*B*). While these values are certainly sufficiently different from those of untreated, precipitated VanX to distinguish the spectrum of the phosphinate complex as being due to a separate chemical species, they suggest a similar chemical structure, *viz.* a five-coordinate species with low axial electronic symmetry, possibly due to a bidentate ligand, and low conformational flexibility compared with the uncomplexed soluble enzyme, probably due to replacement of a water molecule by a rigid ligand. The crystal structure of VanX with bound phosphinate showed that the inhibitor binds through both phosphinate oxygens (1). This mode of binding is entirely consistent with the EPR data.

The EPR spectrum of soluble Co(II)-MBP-VanX treated with phosphinate is markedly different from that of the untreated enzyme and appears to be made up of two components (Fig. 5*A*). Simulations of the major component yielded values very similar to those for phosphinate-treated precipitated VanX: $g_{eff} = 1.83$, 2.78, and 5.82; $E/D = 0.245$; $g_{(x,y)} = 2.252$; $g_{(z)} = 2.177$; and $M_S = |\pm\frac{1}{2}\rangle$. Based on these values, the major species is likely due to the bidentate binding mode of phosphinate to Co(II), similar to that predicted for precipitated Co(II)-VanX with bound inhibitor. The minor component could not be sufficiently well resolved to extract spin Hamiltonian parameters, but the presence of an additional sharp feature at low field suggests that it may be very similar to the major component and that only subtle geometrical differences exist between the two species.

EXAFS Spectra of Zn- and Co(II)-substituted VanX—Fourier-transformed EXAFS spectra for Co(II) and Zn(II)-MBP-VanX are shown in Fig. 6. Both Fourier-transformed EXAFS spectra show a narrowly distributed first shell at ~2.0 Å and outer shell scattering consistent with histidine (imidazole) coordination. Single scattering fits indicate that both cobalt and zinc are coordinated by five nitrogen/oxygen ligands at ~ 2.0 Å (Table II). The size of σ^2 is suggestive of a heterogeneous first coordination sphere, such as the $His_2Asp(OH_2)_2$ coordination indicated above. However, the data lack sufficient resolution to define two independent distances. The average bond lengths are consistent with those expected for five coordination with mixed nitrogen and oxygen ligands (46). The outer shell scattering for the Zn(II) and Co(II) enzymes is remarkably similar, indicating the presence of a pair of His ligands in both forms.[3] Together with the curve fitting results, the similarity of the Zn(II)- and Co(II)-MBP-VanX Fourier-transformed EXAFS spectra demonstrate that zinc and cobalt adopt similar pentacoordinate geometries in the active site of VanX in solution. The similarity of the data further supports the transferability of spectroscopic studies on Co(II)-substituted MBP-VanX to direct investigation of native Zn(II)-VanX.

Comparison of the EXAFS spectra for Co(II)-substituted

[3] A. Costello and D. L. Tierney, unpublished results.

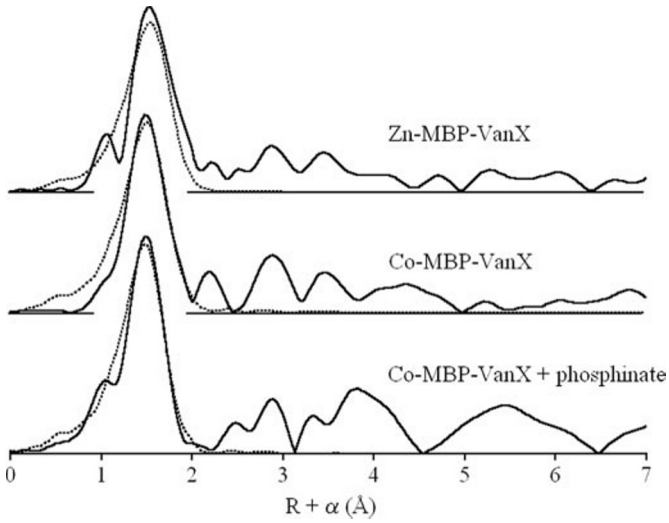

FIG. 6. **Fourier-transformed EXAFS spectra for Zn(II)-MBP-VanX and Co(II)-MBP-VanX in the presence and absence of phosphinate.** First shell fits (*dotted lines*) are reported in Table II.

MBP-VanX with and without the phosphinate analog of D-Ala-D-Ala (Fig. 6) shows extremely similar first shell coordination with a slight decrease in average bond length on inhibitor binding (Table II). Although the two spectra differ dramatically in signal-to-noise ratio, the low R features are sufficiently determined to conclude that the overall coordination number of the Co(II) ion has not changed. The absorption edge energies for Co(II)-substituted MBP-VanX with and without the inhibitor were 7,718.3 eV, strongly suggesting that the coordination numbers about Co(II) in both samples are the same and that the ligand types are similar. Qualitatively the only notable difference in the Fourier-transformed EXAFS spectra below $R + \alpha = 4$ Å is the apparent loss of the outer shell scattering peak at 2.1 Å, a distance consistent with metal-carbon scattering from a coordinated carboxylate (47). Its absence in the inhibitor complex may indicate a shift in, or the loss of, a carboxylate ligand. However, the inhibitor bound data are not of sufficient quality to address this difference quantitatively.

CONCLUSIONS

Based on spectroscopic studies, the metal ion in Co(II)-substituted VanX is five-coordinate. An alternative explanation for the EPR data would require that the $M_S = |\pm\frac{1}{2}\rangle$ spectra observed were, in fact, excited state spectra and that a $M_S = |\pm\frac{3}{2}\rangle$ ground state existed due to tetrahedral Co(II). The observation of only $M_S = |\pm\frac{1}{2}\rangle$ at 8 K would require that such a species exhibited an anomalously low zero field splitting, D. EXAFS analyses returned markedly better fits for 5-fold coordination than for 4-fold coordination, although in the absence of other evidence the assignment could not be taken as unambiguous. Electronic absorption spectroscopy does, however, appear to unambiguously preclude tetrahedral coordination. Taken together then, EXAFS, EPR, and electronic absorption spectroscopy are all consistent only with five-coordinate Co(II) in Co(II)-MBP-VanX.

This result was surprising since the crystal structure of Zn(II)-VanX showed a four-coordinate Zn(II) in the active site of VanX (1). There are at least three possible explanations for this contradictory result. 1) Co(II) in Co(II)-substituted VanX could have a different coordination number than Zn(II). 2) Zn(II) could be coordinated by both carboxylate oxygens of Asp-123, which would be similar to the coordination of Zn(II) by Glu-72 in carboxypeptidase A (45). 3) There could be an additional solvent (or buffer) molecule in VanX that was not reported in the crystal structure (1). Addressing the first expla-

TABLE II
EXAFS fitting results for Zn(II)- and Co(II)-MBP-VanX

Fits shown are to Fourier-filtered data; fits to unfiltered data gave similar results.

Sample	N^a	R_{as}	σ_{as}^{2b}	ΔE_o^c	R^d
		Å			
Zn(II)-MBP-VanX	5 N/O	2.03	4.8	−21	109.0
Co(II)-MBP-VanX	5 N/O	2.00	3.4	−26	12.4
Co(II)-MBP-VanX + phosphinate	5 N/O	1.97	4.1	−18	22.6

[a] Integer coordination number giving the best fit. N/O, nitrogen/oxygen.
[b] Mean square deviation in absorber-scatterer bond length in 10^{-3} Å^2.
[c] The value of ΔE_0 was allowed to vary for Co(II)-MBP-VanX data sets.
[d] Goodness of fit (R) defined as $1000 \times \frac{\sum_{i=1}^{N}\{[\mathrm{Re}(\chi_{i_{calc}})]^2+[\mathrm{Im}(\chi_{i_{calc}})]^2\}}{\sum_{i=1}^{N}\{[\mathrm{Re}(\chi_{i_{obs}})]^2+[\mathrm{Im}(\chi_{i_{obs}})]^2\}}$ where N is the number of data points.

nation, EXAFS studies on Zn(II)-containing and Co(II)-containing VanX demonstrate very clearly that these samples have metal centers with the same coordination number even though there is slight ambiguity as to what precisely this number is. In the literature, there are only two examples of Co(II)-substituted enzymes having a different coordination number than Zn(II) in the native enzyme (48, 49). The likelihood of a substituted Co(II) ion having a higher coordination number than the native Zn(II) is not high when the physiochemical properties of these ions are considered. The ionic radius of Co(II) is 0.02 Å smaller, and the Co(II)-ligand distances are typically shorter than those for native Zn(II) centers (36); these characteristics would argue for Co(II) having a lower coordination number rather than a higher one. The spectroscopic data combined indicate that Co(II) must be five-coordinate in VanX. It is clear on experimental grounds and supported by both theoretical considerations and the extensive literature on Co(II)-substituted Zn(II)-enzymes that Co(II) and Zn(II) in VanX have the same coordination number. Therefore, the evidence indicates that Zn(II) in VanX is five-coordinate.

The crystallographic data reported by Park and co-workers (1) clearly indicate ligands due to His-116 (1 × nitrogen), His-184 (1 × nitrogen), and Asp-123 (1 × oxygen at 2.55 Å). An oxygen atom presumed to be due to water was identified as a fourth ligand. A second oxygen ligand from Asp-123 was modeled at 3.01 Å from Zn(II). Significant differences between the EPR spectra of soluble VanX and precipitated VanX clearly show that the metal center can adopt different geometries depending on the aggregation state of the protein. It must, therefore, be at least considered possible that the second oxygen atom of Asp-123 may adopt a slightly different orientation with respect to Zn(II) in the soluble form of VanX than in the crystalline state, affording a fifth ligand to Zn(II). The precise conformational change required to lengthen the Zn(II)-oxygen bond in the crystalline state will presumably be specific and dependent on the nature of the global conformational change that is necessary to maximize the energetic favorability of the crystal contacts. In contrast, in the precipitated material, there is insufficient driving force to break the Zn–O bond, although the geometry of the site is altered. Although technically difficult, EPR and electronic absorption studies of the crystalline Co(II)-VanX may prove insightful.

The third possible structural scenario consistent with the crystallographic data is that there is a second solvent ligand to Zn(II) in soluble VanX. It is possible, although unlikely, that such a ligand is present in the soluble form but not in the crystalline form. A more likely explanation is that a second solvent ligand may be present in the crystalline form but is undetected. The crystal coordinates were kindly made available for inspection by Dr. Chang H. Park, Abbott Laboratories, and the quality of the data were insufficient to rule out the possibility of an additional solvent ligand, particularly if it were disordered.

In summary, there are rational possible explanations why the crystal structure and the spectroscopic data may initially appear at odds. However, the inescapable conclusion from the spectroscopic work is that Zn(II) in soluble VanX is five-coordinate as is Co(II) in the cobalt-substituted form of the enzyme.

The presence of a five-coordinate Zn(II) or Co(II) in the active site of VanX may have important catalytic consequences. The most stable coordination numbers of Zn(II) or Co(II) in proteins are 4 > 6 > 5 (36). It is likely then that 5-fold coordination of the metal ion represents a state, the entatic state, that is stable in the resting enzyme but is highly reactive toward a hydrolyzable substrate (50). Mechanistic studies on VanX to probe the metal center during catalytic turnover are currently in progress.

Acknowledgment—We thank Professor Chris Walsh of Harvard Medical School for providing the overexpression plasmid for MBP-VanX, pIADL14.

REFERENCES

1. Bussiere, D. E., Pratt, S. D., Katz, L., Severin, J. M., Holzman, T., and Park, C. H. (1998) *Mol. Cell* **2,** 75–84
2. Walsh, C. T. (1999) *Science* **284,** 442–443
3. Walsh, C. T. (1993) *Science* **261,** 308–309
4. Walsh, C. T. (2000) *Nature* **406,** 775–781
5. Walsh, C. T., Fisher, S. L., Park, I. S., Prahalad, M., and Wu, Z. (1996) *Chem. Biol.* **3,** 21–28
6. Williams, D. H., and Bardsley, B. (1999) *Angew. Chem. Int. Ed. Engl.* **38,** 1172–1193
7. Arthur, M., Reynolds, P. E., Depardieu, F., Evers, S., Dutka-Malen, S., Quintiliani, R., and Courvalin, P. (1996) *J. Infect.* **32,** 11–16
8. Holman, T. R., Wu, Z., Wanner, B. L., and Walsh, C. T. (1994) *Biochemistry* **33,** 4625–4631
9. Haldimann, A., Fisher, S. L., Daniels, L. L., Walsh, C. T., and Wanner, B. L. (1997) *J. Bacteriol.* **179,** 5903–5913
10. Ulijasz, A. T., Kay, B. K., and Weisblum, B. (2000) *Biochemistry* **39,** 11417–11424
11. Bugg, T. D. H., Wright, G. D., Dutka-Malen, S., Arthur, M., Courvalin, P., and Walsh, C. T. (1991) *Biochemistry* **30,** 10408–10415
12. Bugg, T. D. H., and Walsh, C. T. (1992) *Nat. Prod. Rep.* 199–215
13. Fan, C., Moews, P. C., Walsh, C. T., and Knox, J. R. (1994) *Science* **266,** 439–443
14. Rao, J., Colton, I. J., and Whitesides, G. M. (1997) *J. Am. Chem. Soc.* **119,** 9336–9340
15. McComas, C. C., Crowley, B. M., and Boger, D. L. (2003) *J. Am. Chem. Soc.* **125,** 9314–9315
16. Reynolds, P. E., Depardieu, F., Dutka-Malen, S., Arthur, M., and Courvalin, P. (1994) *Mol. Microbiol.* **13,** 1065–1070
17. Wu, Z., Wright, G. D., and Walsh, C. T. (1995) *Biochemistry* **34,** 2455–2463
18. McCafferty, D. G., Lessard, I. A. D., and Walsh, C. T. (1997) *Biochemistry* **36,** 10498–10505
19. Lessard, I. A. D., Pratt, S. D., McCafferty, D. G., Bussiere, D. E., Hutchins, C., Wanner, B. L., Katz, L., and Walsh, C. T. (1998) *Chem. Biol.* **5,** 489–504

20. Lessard, I. A. D., and Walsh, C. T. (1999) *Chem. Biol.* **6,** 177–187
21. Lessard, I. A. D., and Walsh, C. T. (1999) *Proc. Natl. Acad. Sci. U. S. A.* **96,** 11028–11032
22. Yang, K. W., Brandt, J. J., Chatwood, L. L., and Crowder, M. W. (2000) *Bioorg. Med. Chem. Lett.* **10,** 1087–1089
23. Wu, Z., and Walsh, C. T. (1995) *Proc. Natl. Acad. Sci. U. S. A.* **92,** 11603–11607
24. Wu, Z., and Walsh, C. T. (1996) *J. Am. Chem. Soc.* **118,** 1785–1786
25. Araoz, R., Anhalt, E., Rene, L., Badet-Denisot, M. A., Courvalin, P., and Badet, B. (2000) *Biochemistry* **39,** 15971–15979
26. Tu, J., and Chu, Y. H. (1998) *Anal. Biochem.* **264,** 293–296
27. Yaouancq, L., Anissimova, M., Badet-Denisot, M. A., and Badet, B. (2002) *Eur. J. Org. Chem.* 3573–3579
28. Rajagopalan, P. T., Grimme, S., and Pei, D. (2000) *Biochemistry* **39,** 779–790
29. Bennett, B., and Holz, R. C. (1997) *J. Am. Chem. Soc.* **119,** 1923–1933
30. Bennett, B. (2002) *Curr. Top. Biophys.* **26,** 49–57
31. Ankudinov, A. L., Ravel, B., Rehr, J. J., and Conradson, S. D. (1998) *Phys. Rev. B: Condens. Matter* **58,** 7565–7576
32. Kolotilov, S. V., Addison, A. W., Trofimenko, S., Dougherty, W., and Pavlishchuk, V. V. (2004) *Inorg. Chem. Commun.* **7,** 485–488
33. McClure, C. P., Rusche, K. M., Peariso, K., Jackman, J. E., Fierke, C. A., and Penner-Hahn, J. E. (2003) *J. Inorg. Biochem.* **94,** 78–85
34. Auld, D. S. (1995) in *Methods Enzymol.*, Vol. 248, pp. 228–241, Academic Press, New York
35. Auld, D. S. (1988) in *Methods Enzymol.*, Vol. 158, pp. 71–79, Academic Press, New York
36. Maret, W., and Vallee, B. L. (1993) in *Methods Enzymol*, Vol. 226, pp. 52–71, Academic Press, New York
37. Garmer, D. R., and Krauss, M. (1993) *J. Am. Chem. Soc.* **115,** 10247–10257
38. Kiefer, L. L., and Fierke, C. A. (1994) *Biochemistry* **33,** 15233–15240
39. Gilson, H. S. R., and Krauss, M. (1999) *J. Am. Chem. Soc.* **121,** 6984–6989
40. Crowder, M. W., Yang, K. W., Carenbauer, A. L., Periyannan, G., Seifert, M. A., Rude, N. E., and Walsh, T. R. (2001) *J. Biol. Inorg. Chem.* **6,** 91–99
41. Andersson, M. E., Hogbom, M., Rinaldo-Matthis, A., Andersson, K. K., Sjoberg, B. M., and Nordlund, P. (1999) *J. Am. Chem. Soc.* **121,** 2346–2352
42. Martinelli, R. A., Hanson, G. R., Thompson, J. S., Holmquist, B., Pilbrow, J. R., Auld, D. S., and Vallee, B. L. (1989) *Biochemistry* **28,** 2251–2258
43. Bennett, B., and Holz, R. C. (1997) *Biochemistry* **36,** 9837–9846
44. D'souza, V. M., Bennett, B., Copik, A. J., and Holz, R. C. (2000) *Biochemistry* **39,** 3817–3826
45. Rees, D. C., Lewis, M., and Lipscomb, W. N. (1983) *J. Mol. Biol.* **168,** 367–387
46. Allen, F. H. (2002) *Acta Crystallogr. Sect. B Struct. Sci.* **58,** 380–388
47. Randall, C. R., Zang, Y., True, A. E., Que, L., Jr., Charnock, J. M., Garner, C. D., Fujishima, Y., Schofield, C. J., and Baldwin, J. E. (1993) *Biochemistry* **32,** 6664–6673
48. Holz, R. C. (2002) *Coord. Chem. Rev.* **232,** 5–26
49. Kleifeld, O., Rulisek, L., Bogin, O., Frenkel, A., Havlas, Z., Burstein, Y., and Sagi, I. (2004) *Biochemistry* **43,** 7151–7161
50. Williams, R. J. (1995) *Eur. J. Biochem.* **234,** 363–381